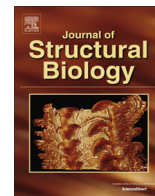




Contents lists available at ScienceDirect

Journal of Structural Biology

journal homepage: www.elsevier.com/locate/yjsbi

Automatic segmentation of high pressure frozen and freeze-substituted mouse retina nuclei from FIB-SEM tomograms

Thai V. Hoang^{a,b,c,d}, Caroline Kizilyaprak^e, Danièle Spehner^{a,b,c,d}, Bruno M. Humbel^e, Patrick Schultz^{a,b,c,d,*}

^a IGBMC (Institut de Génétique et de Biologie Moléculaire et Cellulaire), 1, rue Laurent Fries, BP 10142, 67404 Illkirch, France

^b Inserm, U964, Illkirch, France

^c CNRS, UMR7104, Illkirch, France

^d Université de Strasbourg, Strasbourg, France

^e University of Lausanne, Electron Microscopy Facility, 1015 Lausanne, Switzerland

ARTICLE INFO

Article history:

Received 4 February 2016

Received in revised form 3 October 2016

Accepted 6 October 2016

Available online xxxxx

Keywords:

FIB/SEM tomography

Segmentation

Nucleus

Heterochromatin

ABSTRACT

Focused Ion Beam milling combined with Scanning Electron Microscopy is a powerful tool to determine the 3-D organization of whole cells and tissue at an isotropic resolution of 3–5 nm. This opens the possibility to quantify several cellular parameters and to provide detailed phenotypic information in normal or disease states. Here we describe Biocomputing methods to extract in an automated way characteristic features of mouse rod photoreceptor nuclei such as the shape and the volume of the nucleus; the proportion of heterochromatin; the number, density and distribution of nuclear pore complexes (NPC). Values obtained on five nuclei show that the number of NPC (348 ± 8) is the most conserved feature. Nuclei in higher eukaryotes show large variations in size and rod nuclei are amongst the smallest reported ($32 \pm 3 \mu\text{m}^3$). Despite large species- and cell-type-specific variations in size, the density of NPC (about $15/\mu\text{m}^2$) is highly conserved.

© 2016 Elsevier Inc. All rights reserved.

1. Introduction

The internal organization of cells reflects the expressed part of their genome, determines their specialized role in different tissues, and notifies about their physiological or pathological state. Since the first electron micrograph of cells using transmission electron microscopy (TEM) in 1945 (Porter et al., 1945), electron microscopy (EM) methods have continually improved our appreciation of complex levels of cellular organization. The high spatial resolution of electron microscopes produces a wealth of information about the structure, distribution and interactions between cellular organelles. Early electron microscopy observations of cellular structures were essentially two-dimensional (2-D) and resulted in mostly descriptive information. Stereological methods were used to predict or estimate the size and distribution of cellular structures by extrapolating from 2-D measurements to the whole cellular volume (Weibel et al., 1966). To circumvent limitations due to the intricate shape of cellular structures which prevents straightforward extrapolation, new methods were developed to retrieve 3-D information from cellular samples. By sequentially

tilting the specimen relative to the electron beam, TEM tomography produces a 3-D model of a cell section (Hoppe and Grill, 1977). This powerful method is however limited to 500 nm in the Z-depth by section thickness and the reconstruction of an entire eukaryotic cell can be very challenging (Noske et al., 2008). Serial thin sections and TEM imaging can solve the problem of the limited Z-depth but this technique is very labor intense and needs highly skilled experimenters (Porter and Blum, 1953; White et al., 1986; Bumbarger et al., 2013). The technological challenge for rapid 3-D imaging of large mammalian cells at nanometric scale was first met with the introduction of block face imaging with a scanning electron microscope (SEM). In this case, the block face of an embedded sample is imaged with sufficient resolution and depth discrimination using the back scattered electron (BSE) detectors. To obtain 3-D data, the block face needs to be repeatedly imaged, with the top slice removed between image acquisitions. One possibility is to remove the top slice with an ultramicrotome in the chamber of a SEM (serial block face, SFB-SEM). This method was introduced 30 years ago by Leighton who constructed a microtome for cutting sections inside the microscope chamber (Leighton, 1981). More recently, Denk and Horstmann showed that with a custom-designed microtome in a SEM, 3-D ultrastructural data can be obtained at the resolution and with a volume sufficient to follow local neuronal circuits (Denk and Horstmann, 2004).

* Corresponding author at: IGBMC (Institut de Génétique et de Biologie Moléculaire et Cellulaire), 1, rue Laurent Fries, BP10142, 67404 Illkirch, France.

E-mail address: patrick.schultz@igbmc.fr (P. Schultz).

Currently, the Z-resolution of SBF-SEM of about 25 nm is limited by the minimal section thickness that can be cut with a diamond-knife (Friedrich et al., 2013; Kasthuri et al., 2007; Tapia et al., 2012). The removal of top slices in smaller increments can also be performed by focused gallium ion beam (FIB) milling (Heymann et al., 2006). Recently, the limits of FIB-SEM tomography were pushed to create high-resolution $5 \times 5 \times 5$ nm isotropic voxel acquisition on $40 \times 40 \mu\text{m}$ large image areas and over a depth of several tenths of micrometers (Narayan et al., 2014; Wei et al., 2012). The combination of focused ion beam (FIB) milling and block-face SEM imaging (FIB-SEM tomography) has become a powerful tool for 3-D investigation of cellular ultrastructure and constitutes currently one of the most fast-growing methods to obtain undistorted volume information (Bosch et al., 2015; Cretoiu et al., 2015; De Winter et al., 2009; Hekking et al., 2009; Heymann et al., 2009; Knott et al., 2008; Merchán-Pérez et al., 2009). This new imaging technology opens the possibility to measure morphological parameters on discrete ultrastructural feature. Along with these large 3-D image stacks come many computational challenges to achieve automated 3-D object recognition, annotation, data integration, representation and exploitation. Segmentation is central to these tasks and corresponds to the process of partitioning the 3-D images into multiple structurally defined regions to produce a more meaningful representation suitable for quantitative analysis. This process can be used to delineate the boundaries between cellular compartments or between organelles and cytosol so that quantitative information such as the size, distribution, surface morphology can be extracted from these delineated regions.

Many segmentation techniques have been proposed to target nature scene and medical images. These techniques usually group nearby pixels into regions by optimizing a target function that prefers pixels in the same group to have similar intensity levels and at the same time expects a small number of groups (Arbelaez et al., 2011; Van den Bergh et al., 2014). In spite of many successful applications, these techniques are not suitable for electron microscopy images because of their low signal-to-noise ratio, low contrast and complex image contents. For example, in the presence of noise the performance of watershed transform-based methods (Coupré et al., 2011) decreases rapidly since noise changes the topological landscape of the intensity function representing the image contents and thus breaks biologically-meaningful regions into many small fragments. Recently, some research groups have developed algorithms and software tools that can aid the segmentation of electron microscopy images automatically (Nunez-Iglesias et al., 2014; Schindelin et al., 2012). For boundary segmentation, membrane signals are usually enhanced by filtering and then traced by thresholding (Martínez-Sánchez et al., 2014). For region segmentation, a superpixel-based method is often used to over-segment the image and then a split-and-merge strategy is used for region grouping (Jones et al., 2015). A classifier trained with human annotated data can also be used for direct pixel classification (Sommer et al., 2011). These methods were mostly developed for segmentation of brain tissue images with 25 nm resolution in the Z-direction. However, most of the developed segmentation algorithms work only with 2-D images and much human effort is still required to correct the automated segmentation results.

Here we have developed algorithms and software tools in a high-throughput computational workflow covering image preprocessing, semi-automatic segmentation of cell nuclei, and extraction of quantitative data from 3-D FIB-SEM images of murine rod photoreceptor cell nuclei. How our genetic information is organized in the cell nucleus and how this organization affects nuclear function are major questions in the chromatin field which remain largely unanswered. In eukaryotes, the genetic information is

packaged through a hierarchy of folding events. At the first level DNA is wrapped around an histone octamer to form the nucleosome core particle whose atomic structure is defined (Luger et al., 1997). The fundamental repeated element of chromatin, the nucleosome, is composed of the core particle flanked by linker DNA which connects successive nucleosomes and variable amounts of linker histone H1. Purified chromatin appears as an extended 11-nm fiber formed by a linear beads-on-a-string nucleosomal array that compacts into 30 nm fibers in physiological ionic strength and in the presence of histone H1 (Oudet et al., 1975; Thoma et al., 1979). Direct electron microscopy imaging of nuclear sections described highly compact electron dense heterochromatin (HC) compartments and more extended euchromatin (EC) territories but has provided little information on chromatin organization beyond the nucleosomal level and in particular has not confirmed the 30-nm fibers as the fundamental *in vivo* secondary structure of chromatin (Bouchet-Marquis et al., 2005; Horowitz-Scherer and Woodcock, 2005). However, recent publications provide evidence that 30 nm chromatin fibers may exist in highly condensed chromatin states (Kizilyaprak et al., 2010). The chromatin organization in intact nuclei is thus still a matter of debate.

The tools developed here extend previous quantification efforts of nuclear structures (Rouquette et al., 2009) and assign automatically the extent of the nuclear envelope and measure the size of the nuclei as well as its elongation. The nuclear envelope is perforated by nuclear pores that regulate the exchanges between the nucleus and the cytoplasm. The number and distribution of the pores are determined automatically without using correlation methods. Finally the highly condensed heterochromatin compartment is identified automatically thus opening the possibility to model the rheology of the nucleus within its numerous channels or the diffusion of transcription factors within the nuclei.

2. Results

2.1. Data collection

To address the quantification of ultrastructural features and particularly the very sensitive nuclei considerations have to be given concerning sample preparation in order to image cells in their closest to native state. In this study, we used high-pressure freezing (HPF) and freeze-substitution (FS) to prepare 4-days old mice retina samples. High-pressure freezing is a method of choice to obtain optimal structural preservation of bulk biological samples with minimal structural rearrangements (Moor et al., 1980). During freeze substitution cryo-immobilized samples were dehydrated by exchange of ice against an organic solvent at low temperature (-90°C) and then embedded in resin (Humbel et al., 1983; Humbel and Schwarz, 1989). High pressure-frozen and freeze-substituted mouse rod photoreceptor nuclei were observed by FIB-SEM tomography and a 3-D images stack was recorded with resolutions of 3.92 nm, 3.92 nm, 5.00 nm in the X, Y, and Z directions, respectively. The stack contained five complete nuclei that were further analyzed to extract quantitative morphological information (Fig. 1A and 7A).

2.2. Image pretreatment

Successive images were aligned and their grey-level intensity was normalized. After preprocessing, the images still showed density variations that are not related to the structure of the sample but are detrimental for subsequent image segmentation. A global effect is observed as a continuous intensity variation over the whole imaged area best evidenced in false colors (Fig. 1B). This defect might arise from the SEM optics or variations in secondary

Download English Version:

<https://daneshyari.com/en/article/5591550>

Download Persian Version:

<https://daneshyari.com/article/5591550>

[Daneshyari.com](https://daneshyari.com)